

Magnetic switching driven by nanosecond scale heat and magnetic field pulses: An application of macrospin Landau-Lifshitz-Bloch model

U Kilic, G Finocchio, Thomas Hauet, G Aktas, S.H. Florez, Ozhan Ozatay

► **To cite this version:**

U Kilic, G Finocchio, Thomas Hauet, G Aktas, S.H. Florez, et al.. Magnetic switching driven by nanosecond scale heat and magnetic field pulses: An application of macrospin Landau-Lifshitz-Bloch model. Applied Physics Letters, American Institute of Physics, 2012, 10.1063/1.4772486 . hal-01345392

HAL Id: hal-01345392

<https://hal.archives-ouvertes.fr/hal-01345392>

Submitted on 13 Jul 2016

HAL is a multi-disciplinary open access archive for the deposit and dissemination of scientific research documents, whether they are published or not. The documents may come from teaching and research institutions in France or abroad, or from public or private research centers.

L'archive ouverte pluridisciplinaire **HAL**, est destinée au dépôt et à la diffusion de documents scientifiques de niveau recherche, publiés ou non, émanant des établissements d'enseignement et de recherche français ou étrangers, des laboratoires publics ou privés.

Magnetic switching driven by nanosecond scale heat and magnetic field pulses: An application of macrospin Landau-Lifshitz-Bloch model

U. Kilic, G. Finocchio, T. Hauet, S. H. Florez, G. Aktas et al.

Citation: *Appl. Phys. Lett.* **101**, 252407 (2012); doi: 10.1063/1.4772486

View online: <http://dx.doi.org/10.1063/1.4772486>

View Table of Contents: <http://apl.aip.org/resource/1/APPLAB/v101/i25>

Published by the [American Institute of Physics](http://www.aip.org).

Related Articles

Nanosecond-range multi-pulses synchronization based on magnetic switch and saturable pulse transformer
Rev. Sci. Instrum. **83**, 124703 (2012)

Metastable state in a shape-anisotropic single-domain nanomagnet subjected to spin-transfer-torque
Appl. Phys. Lett. **101**, 162405 (2012)

In situ magnetic force microscope studies of magnetization reversal of interaction domains in hot deformed Nd-Fe-B magnets
J. Appl. Phys. **111**, 103901 (2012)

Reversible switching of room temperature ferromagnetism in CeO₂-Co nanoparticles
Appl. Phys. Lett. **100**, 172405 (2012)

Switching through intermediate states seen in a single nickel nanorod by cantilever magnetometry
J. Appl. Phys. **111**, 083911 (2012)

Additional information on *Appl. Phys. Lett.*

Journal Homepage: <http://apl.aip.org/>

Journal Information: http://apl.aip.org/about/about_the_journal

Top downloads: http://apl.aip.org/features/most_downloaded

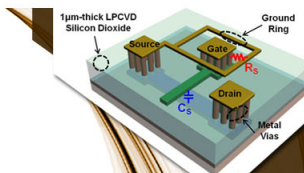
Information for Authors: <http://apl.aip.org/authors>

ADVERTISEMENT



**EXPLORE WHAT'S
NEW IN APL**

SUBMIT YOUR PAPER NOW!



SURFACES AND INTERFACES

Focusing on physical, chemical, biological, structural, optical, magnetic and electrical properties of surfaces and interfaces, and more...



ENERGY CONVERSION AND STORAGE

Focusing on all aspects of static and dynamic energy conversion, energy storage, photovoltaics, solar fuels, batteries, capacitors, thermoelectrics, and more...

Magnetic switching driven by nanosecond scale heat and magnetic field pulses: An application of macrospin Landau-Lifshitz-Bloch model

U. Kilic,^{1,2} G. Finocchio,³ T. Hauet,⁴ S. H. Florez,⁵ G. Aktas,¹ and O. Ozatay¹

¹Department of Physics, Bogazici University, Bebek 34342, Istanbul, Turkey

²Electrical and Electronics Engineering Department, Istanbul Bilgi University, 34060, Istanbul, Turkey

³Department of Electronic Engineering, Industrial Chemistry and Engineering, University of Messina, I-98166 Messina, Italy

⁴Institut Jean Lamour, Université de Lorraine-CNRS UMR 7198, Nancy, France

⁵HGST (Western Digital Company), San Jose Research Center, San Jose, California 95135, USA

(Received 20 September 2012; accepted 3 December 2012; published online 19 December 2012)

High-temperature (near Curie-point) magnetization-behavior in materials with strong-perpendicular-magnetocrystalline-anisotropy has recently gained importance due to potential applications in thermally/heat-assisted-magnetic-recording (TAR/HAMR) systems. We have implemented a macrospin-model within the Landau-Lifshitz-Bloch formalism for strongly exchange-coupled CoNi/Pd multilayers subject to nanosecond-scale localized-heat and magnetic-field pulses. The temperature dependence of the longitudinal-susceptibility, as determined from a single-fitting-parameter of the experimental coercive-field, is consistent with the previously reported *ab initio* calculations. We demonstrate that this model is able to predict the full map of switching-speed as a function of magnetic-field and local-temperature providing a robust tool for the evaluation of this and similar material systems in TAR/HAMR applications. © 2012 American Institute of Physics.

[<http://dx.doi.org/10.1063/1.4772486>]

One of the key issues that a magnetic recording technology has to address is the ultra-high data storage density, which needs to be realized with a low cost production technique. An implementation of such a magnetic memory device can potentially be achieved with the use of magnetic multilayer (ML) thin films that possess strong perpendicular magnetic anisotropy, which creates thermal stability necessary for practical applications. On the other hand, significant improvements in the thermal stability bring other challenges involving the write operation, namely the need to apply high magnetic fields not available with conventional writing heads. In an attempt to overcome this obstacle, thermally/heat assisted magnetic recording (TAR/HAMR) based on magnetization switching at temperatures close to the Curie point (T_c) has been proposed as a viable solution.¹⁻⁴ This has brought the relatively unexplored territory of switching dynamics in the vicinity of the ferromagnet/paramagnet phase transition point into focus. Data storage densities over few Tb/in.² will be attainable once the technical difficulties on the route to a reliable heat assisted writing scheme are identified and resolved. Particularly, in-depth understanding of the underlying physics of magnetic recording at elevated temperatures (close to the phase transition point) will be crucial.

The write stage in the TAR/HAMR process consists of a sequential application of a localized laser pulse (heating pulse) and a writing magnetic field pulse, whose magnitude is larger than the coercivity of the heated region in order to ensure magnetization reversal. The purpose of localized heating is to momentarily decrease the coercive field, allowing an energy-efficient write process, while maintaining high thermal stability at the ambient temperature. CoNi/Pd multilayer structure has an inherently strong magnetocrystalline perpendicular anisotropy. However, similar to the case of FePt, the strong perpendicular anisotropy diminishes at the phase transition point and can be recovered upon cooling to

a temperature far below the Curie point.^{1,5} It is paramount to grasp the details of the magnetization switching process close to T_c to be able to assess the physical limitations inherently imposed on the recording speed as well as to optimize material dependent factors that determine the ultimate magnetic memory device performance.

The conventional approach to study the magnetization dynamics from a broader perspective is based on the solution of the Landau-Lifshitz-Gilbert (LLG) equation where the finite temperature effects are included through an effective stochastic Langevin field term.^{6,7} This formalism has been applied in micromagnetic simulations for decades and has proven very effective in describing the magnetic excitations for low temperatures far from T_c .

On the other hand, the LLG formalism has proven inapplicable to problems involving ultrafast changes in temperature (induced by laser pulses), coupled with applied magnetic field pulses, which trigger the reversal process as envisioned in TAR/HAMR applications.^{4,8-10} The main limitation of the LLG based micromagnetic approach for this regime is the incorrect assumption of conservation of magnetization length during the dynamical excitations. In fact, the field driven transverse fluctuations are accompanied by the rapid temperature change induced longitudinal fluctuations in the magnetization length. The longitudinal fluctuations have their own relaxation characteristics and need to be represented by a temperature dependent longitudinal damping term in the model. The recognition of this issue has led to the development of the Landau-Lifshitz-Bloch (LLB) equation by means of the reduction of the Fokker-Planck equation in the mean field approximation.¹¹ Moreover, the Gaussian stochastic processes as a result of the thermal excitations of magnetic moments in contact with the heat bath have been included to satisfy the well-known Boltzmann statistics at the high temperature limit, resulting in the

stochastic form of the LLB equation (s-LLB).⁸ Many relevant experimental findings such as ultrafast demagnetization have already been demonstrated to be consistent with the LLB prediction.¹²

In this study, we report on an LLB based macrospin model applied to a CoNi/Pd magnetic ML thin film to extract the temperature dependent switching behavior with realistic input parameters identified from experimental data. Previous studies on L1₀ phase FePt relied upon material parameters determined from *ab initio* calculations.^{4,9,10}

The CoNi/Pd MLs were sputter deposited onto a Si/SiO₂ substrate with a stack consisting of Ta (1.5 nm)/Pd (3 nm)/[Co₅₅Ni₄₅ (0.22 nm)/Pd (1.2 nm)] × 22 repeats/Pd (2 nm). The films exhibited strong perpendicular anisotropy field H_k = 18 kOe (corresponding to ~2 × 10⁶ erg/cm³) and saturation magnetization M_s = 220 emu/cm³ as determined from vibrating specimen magnetometry (VSM) measurements at room temperature. A striking feature of such magnetic material systems is the strong exchange coupling (exchange lengths in the 20-30 nm range with an effective exchange constant A = 3 – 6 × 10⁻⁶ ergs/cm (Ref. 1)), which makes them a good candidate for macrospin like switching behaviour in granular thin films or bit patterned media. Figs. 1(a) and 1(b) show the temperature dependence of the M_s (curve for H = 0 Oe) and the coercive field as measured with the VSM technique, respectively. The T_c was measured to be 448 K and an estimate of the zero temperature equilibrium magnetization was obtained as 250 emu/cm³ from extrapolation to zero temperature in the data of Fig. 1(a) (where an out of plane magnetic field of 1 kOe was applied to avoid demagnetization by breaking into domains above 400 K).

The LLB formalism adopted is a generalized equation of motion for magnetization dynamics of classical and quantum ferromagnets,¹¹ which takes into account the longitudinal excitations in addition to transverse components during the time evolution of magnetization. The s-LLB as written for a macrospin describes the time evolution of the average magnetization $\mathbf{m} = \mathbf{M}/M_s(T=0)$ (\mathbf{M} is the magnetization vector)

$$\frac{\partial \mathbf{m}}{\partial t} = -\tilde{\gamma}(\mathbf{m} \times \mathbf{H}_{\text{eff}}) + \frac{\tilde{\gamma}\alpha_{//}}{|\mathbf{m}|^2}[\mathbf{m} \cdot (\mathbf{H}_{\text{eff}})]\mathbf{m} - \frac{\tilde{\gamma}\alpha_{\perp}}{|\mathbf{m}|^2}\mathbf{m} \times [\mathbf{m} \times (\mathbf{H}_{\text{eff}} + \boldsymbol{\zeta}_{\perp})] + \boldsymbol{\zeta}_{//}, \quad (1)$$

Where $\tilde{\gamma}$ is the absolute value of the gyromagnetic ratio; \mathbf{H}_{eff} is the effective magnetic field; $\alpha_{//}$ and α_{\perp} are the longitudinal and transverse damping parameters, respectively; $\boldsymbol{\zeta}_{//}$ and $\boldsymbol{\zeta}_{\perp}$ are, respectively, the longitudinal torque and the transverse effective field terms due to Gaussian stochastic thermal fluctuation processes.⁸ The temperature dependence of the transverse and longitudinal damping parameters are given by

$$\alpha_{//} = \alpha_G \left(\frac{2T}{3T_c} \right); \quad \alpha_{\perp} = \begin{cases} \alpha_G \left(1 - \frac{T}{3T_c} \right) & T < T_c \\ \alpha_G \left(\frac{2T}{3T_c} \right) & T \geq T_c \end{cases}, \quad (2)$$

where α_G is the weakly temperature dependent macroscopic Gilbert damping parameter whose value was estimated to be 0.0275.¹³⁻¹⁶ The effective field consists of the following components:⁸

$$\mathbf{H}_{\text{eff}} = \mathbf{H}_{\text{appl}} + \mathbf{H}_{\text{an}} + \begin{cases} \frac{1}{2\chi_{//}} \left(1 - \frac{m^2}{m_e^2} \right) \mathbf{m}, & T \leq T_c \\ \frac{1}{2\chi_{//}} \left[\frac{3}{5} \left(\frac{T_c}{T_c - T} \right) m^2 - 1 \right] \mathbf{m} & T \geq T_c \end{cases}, \quad (3)$$

where \mathbf{H}_{appl} is the applied field, \mathbf{H}_{an} is the anisotropy field, and the last term is the longitudinal effective field which is a function of material and temperature dependent longitudinal susceptibility $\chi_{//}$ and zero field equilibrium magnetization m_e .^{3,9,10,17} Finally, the stochastic terms satisfy the following relations:

$$\begin{cases} \langle \zeta_i^{//}(0) \zeta_j^{\perp}(t) \rangle = \left(\frac{2k_B T (\alpha_{\perp} - \alpha_{//})}{\mu_0 |\gamma| \Delta V M_s \alpha_{\perp}^2} \right) \delta_{ij} \delta(t) \\ \langle \zeta_i^{//}(0) \zeta_j^{//}(t) \rangle = \left(\frac{2k_B T |\gamma| \alpha_{//}}{\Delta V M_s} \right) \delta_{ij} \delta(t) \\ \langle \zeta_i^{//} \zeta_j^{\perp} \rangle = 0 \\ \langle \zeta^{\mu} \rangle_{\mu=\perp, //} = 0 \end{cases}, \quad (4)$$

Where k_B is the Boltzman constant, μ_0 is the permeability of free space, ΔV is the volume of the computational cubic cell,

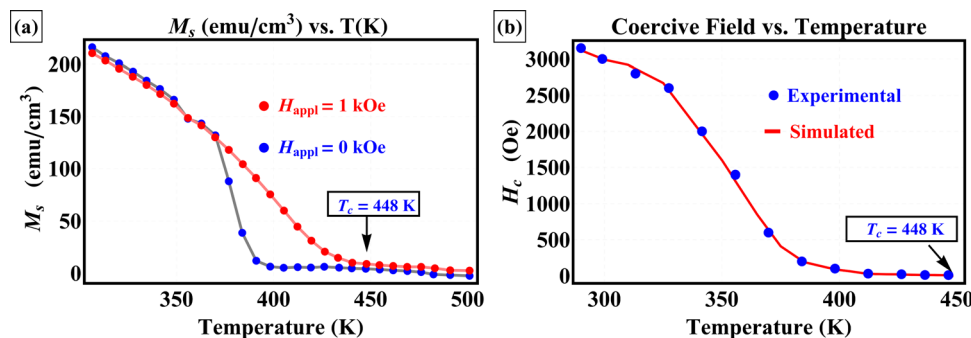


FIG. 1. Temperature dependence of both saturation magnetization and coercivity by using VSM measurement technique and extraction of temperature dependence of longitudinal susceptibility by inserting the coercivity values as applied external field to the system. (a) Temperature dependence of saturation magnetization measured in the existence of an out of plane magnetic field (red color) and with no field (blue color). (b) Temperature dependence of coercivity obtained from the hysteresis loops at different temperatures (point markers), solid line simulations. Reprinted with permission from Appl. Phys. Lett. 95, 172502 (2009). Copyright 2009 American Institute of Physics.

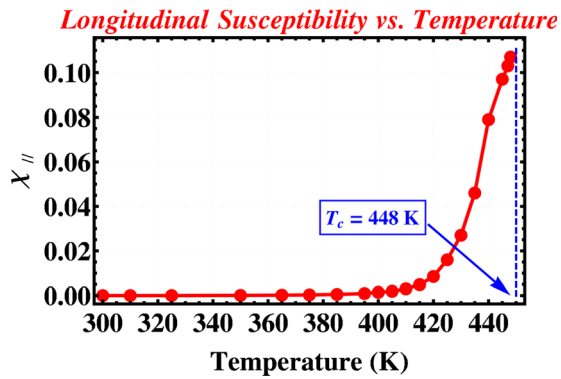


FIG. 2. Extraction of temperature dependence of longitudinal susceptibility. Susceptibility as a function of temperature extracted from the LLB simulations.

$\tilde{\gamma} = \frac{\gamma}{1+\alpha_G^2}$, i and j represent spatial components in Cartesian coordinates x , y , and z .

The point markers of Figure 1(b) show the temperature dependence of the coercive field obtained from magnetization vs. magnetic field hysteresis loop measurements taken at several different temperatures in the 300 K to 450 K range. Using the longitudinal susceptibility ($\chi_{||}$) as a single fit parameter, the magnetic field required for switching of the CoNi/Pd ML (the coercive field H_c), as computed from macrospin LLB simulations, was matched to the experimental values for each temperature and interpolated to a continuous function as shown by the solid line in Figure 1(b). Figure 2 displays the resulting longitudinal susceptibility as a function of temperature (point markers) together with an interpolating function (solid line). As expected, the longitudinal susceptibility becomes significant in the vicinity of the Curie point confirming that the longitudinal relaxation mechanism implemented in the LLB formalism has indeed gained importance in this regime. In addition, the extracted temperature dependence of the longitudinal susceptibility shows good agreement with computations obtained from *ab initio* calculations,^{9,10,17} indicating a simple experimental way to determine this parameter within the LLB framework.

In an attempt to further improve the understanding of the underlying physics of magnetic recording at elevated temperatures, we investigated the switching properties near the T_c . Figure 3(a) shows the time evolution of normalized (by zero temperature saturation magnetization $M_s(T=0\text{ K}) = 250\text{ emu/cm}^3$) magnetization vector components (blue solid line z component, black solid line y component, and brown solid line x component) together with the magnetization length (red solid line) as response to the application of heating and field pulses. The heating pulse increases the local temperature to 415 K (ambient temperature 300 K) for 1.25 ns. This is followed by a field pulse (with a 0.5 ns delay) that is applied in the $+z$ direction and has 2 kOe amplitude and 1.25 ns width (between 50% transition points). To avoid numerical artifacts in calculations, all pulses had finite rise and fall times of 0.25 ns (defined between 10% and 90% of the transition) (see Ref. 18 for more details about the integration time solver). The increasing relative change in the magnetization length for increasing temperature difference with the ambient is displayed in the inset of Fig. 3(a). The corresponding macrospin trajectory is shown in Fig. 3(b). In these simulations, the initial position of the magnetization vector is slightly tilted (5°) from $-z$ direction (the easy axis determined by the strong perpendicular anisotropy). Therefore, the turn on of a heating pulse followed by a writing field pulse produces a complex trajectory of the magnetization switching with precessional dynamics¹⁹ due to the applied magnetic field and the longitudinal relaxation related to the thermal fluctuations. The effects of thermally induced noise are significant close to T_c . The trajectory is also slightly elliptically due to thin film demagnetizing field effect. We have systematically investigated the switching process as a function of the heating pulse and writing field pulse amplitudes for 1.25 ns pulse width and 0.25 ns rise and 0.25 ns fall times for both heating and writing field pulses and with 0.5 ns delay in between the pulses as shown in Figure 4(a). In our prior work¹ utilizing the experimentally determined temperature dependence of thermal conductivity in the finite element calculations, the thermal relaxation time for CoNi/Pd ML system was estimated to be on the order of 100 ps

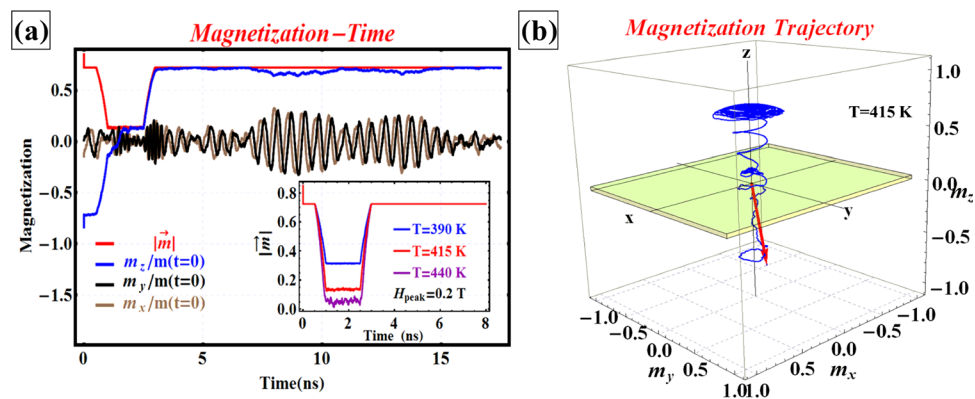


FIG. 3. Modeling of magnetization response to a constant amplitude field pulse and heating pulses with different amplitudes. The visualization of magnetization reversal mechanism as it is driven by LLB equation. (a) The time evolution of magnetization vector components and the magnetization magnitude in the presence of a field pulse with a peak value ($H_{\text{peak}} = 2\text{ kOe}$) and a heating pulse with a peak value ($T_{\text{peak}} = 400\text{ K}$). The duration of pulses is 1.25 ns (50%–50%) and the delay between heating and field pulses is 0.5 ns. The inset shows the time evolution of magnetization magnitude for different temperatures but for the same field amplitude (2 kOe). (b) 3D representation of the magnetization trajectory as it is under the influence of 1.25-ns magnetic field (with 2 kOe peak value) and heating (with 400 K peak value) pulses. While the brown arrow shows the direction of the applied field pulse, the red arrow shows the initial position of the magnetization vector.

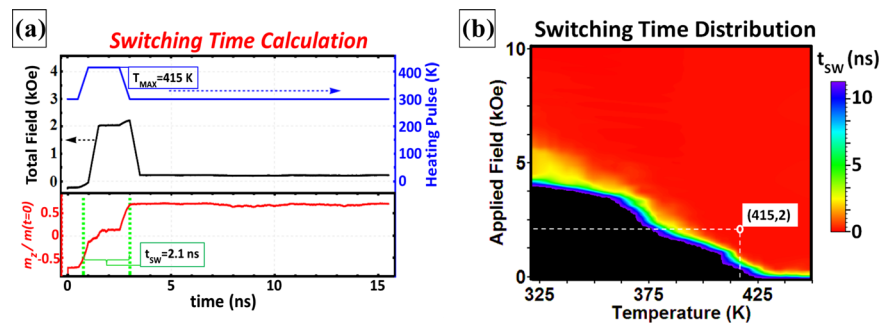


FIG. 4. A simple representation of switching time calculation and switching time distribution for different applied heat and field pulse combinations. (a) Example of switching time calculation for the white point on this figure. While blue and black colors show heating pulse and total effective field ($H_{\text{pulse}} + H_{\text{demag}} + H_{\text{stoc}}$), respectively, the red one is the time evolution of z component of magnetization vector. t_{sw} is the switching time. (b) Switching time analysis when stochasticity is taken into account. Color gradient shows the switching time distribution. In addition to this, black color is showing the non-switching region. While the x axis shows the magnitude of heating pulse, the y axis shows the amplitude of field pulse. For each combination, the width of the peak value of pulses is 1.25 ns.

which is comparable to the typical electron-lattice thermal relaxation time.¹⁰ In order to ensure complete cooling to the ambient temperature, we used 250 ps cooling time in our simulations. The switching time is defined as the time elapsed between the onset of the heating pulse and the instant when 90% of the equilibrium magnetization value is achieved. It is important to note that since the actual switching calculation is intermixed with longitudinal relaxation both during heating and cooling, the switching time obtained with this procedure is merely an upper bound.

Finally, Figure 4(b) shows the calculated switching times as a function of the heating pulse and writing pulse amplitude (averaged over 200 iterations). The switching times are color coded such that the black color implies no switching and red color implies ultrafast switching. Our numerical experiment shows that for a given heating pulse, the switching time can be reduced by applying magnetic fields well above the coercive field value. Most importantly also for temperatures above 425 K (close to $T_c = 448$ K), the ultrafast switching (sub-ns scale) is observed with very small magnetic fields in the order of less than an Oersted. Given that there have been many reports on ultrafast manipulation of magnetization,^{12,20} the actual switching time is expected to be controllable down to 10–100s of fs. Figure 4(b) suggests that at any temperature by over driving the switching with an applied field higher than the coercive field the switching time can be reduced to sub-nanosecond scale.

In summary, we have implemented a comprehensive macrospin LLB model to understand the nature of switching dynamics in CoNi/Pd MLs close to Curie temperature. Consistent with previous reports, an enhanced damping is observed by increasing the temperature of the magnetic medium which leads to an increase in the switching speed. We find that ultrafast switching is attainable as long as heating pulses allow the medium to reach temperature sufficiently close to the phase transition point. Furthermore, employing experimentally determined temperature dependence of CoNi/Pd ML intrinsic parameters in LLB calculations the longitudinal relaxation behaviour, which plays a major role in the elevated temperature dynamics, is quantifiable by using longitudinal susceptibility as a single fit parameter to match the calculated switching fields to the experimental

values. The results obtained with our method show good agreement with prior studies involving *ab initio* calculations. While using a simple macrospin approach appears effective in describing the average behaviour of strongly exchange-coupled magnetic MLs, a good understanding of the detailed switching mechanism and the role of geometry when patterned into nanoscale structures would necessitate an extension of our model to micromagnetic simulations. Nevertheless, this simple approach allows evaluation of the switching properties of CoNi/Pd MLs with a relatively low Curie temperature and strong perpendicular anisotropy at room temperature and other similar thin film structures as a candidate for granular or bit patterned TAR/HAMR applications.

This work is supported by Bogazici University Research Fund under the Contract Nos. 5051 and 6121, the Scientific and Technological Research Council of Turkey (TUBITAK) under the Contract No. 112T205, and the Turkish Academy of Sciences TUBA-GEBIP Award. G.F. was supported by the Spanish Project under Contract No. MAT2011-28532-C03-01. The authors thank Dmitry Garanin, Unai Atxitia Macizo, and Oksana Chubykalo-Fesenko Morozova for helpful discussions.

¹O. Ozatay, T. Hauet, S. H. Florez, J. A. Katine, A. Moser, J.-U. Thiele, L. Folks, and B. D. Terris, *Appl. Phys. Lett.* **95**, 172502 (2009).

²O. Ozatay, P. G. Mather, J.-U. Thiele, T. Hauet, and P. M. Braganca, *Handbook of Nanoscale Optics and Electronics*, Ch.4 Spin-Based Data Storage (Elsevier B.V., 2010).

³K. Nagata, Y. Kawakubo, D. Kato, and T. Sugiyama, in *Digest of the 2002 Asia-Pacific Magnetic Recording Conference*, Singapore (IEEE, 2002).

⁴T. W. McDaniel, *J. Appl. Phys.* **112**, 013914 (2012).

⁵T. Bublat and D. Goll, *J. Appl. Phys.* **108**, 113910 (2010).

⁶W. F. Brown, Jr., *Phys. Rev.* **130**, 1677–1686 (1963).

⁷G. Finocchio, I. N. Krivorotov, X. Cheng, L. Torres, and B. Azzaroni, *Phys. Rev. B* **83**, 134402 (2011).

⁸R. F. L. Evans, D. Hinzke, U. Atxitia, U. Nowak, and R. W. Chantrell, *Phys. Rev. B* **85**, 014433 (2012).

⁹O. Chubykalo-Fesenko, U. Nowak, R. W. Chantrell, and D. Garanin, *Phys. Rev. B* **74**, 094436 (2006).

¹⁰U. Atxitia and O. Chubykalo-Fesenko, *Appl. Phys. Lett.* **91**, 232507 (2007).

¹¹D. Garanin, *Phys. Rev. B* **55**, 3050 (1997).

¹²U. Atxitia, O. Chubykalo-Fesenko, J. Walowski, A. Mann, and M. Müntenberg, *Phys. Rev. B* **81**, 174401 (2010).

- ¹³Z. R. Tadisina, A. Natarajathinam, B. D. Clark, A. L. Highsmith, T. Mewes, S. Gupta, E. Chen, and S. Wang, *J. Appl. Phys.* **107**, 09C703 (2010).
- ¹⁴D. Stanescu *et al.*, *J. Appl. Phys.* **103**, 07B529 (2008).
- ¹⁵S. Mizukami, X. Zhang, T. Kubota, H. Naganuma, M. Oogane, Y. Ando, and T. Miyazaki, *Appl. Phys. Express* **4**, 013005 (2011).
- ¹⁶S. Pal, B. Rana, O. Hellwig, T. Thomson, and A. Barman, *Appl. Phys. Lett.* **98**, 082501 (2011).
- ¹⁷C. Schieback, D. Hinzke, M. Klaui, U. Nowak, and P. Nielaba, *Phys. Rev. B* **80**, 214403 (2009).
- ¹⁸A. Giordano, G. Finocchio, L. Torres, M. Carpentieri, and B. Azzarboni, *J. Appl. Phys.* **111**, 07D112 (2012).
- ¹⁹C. Serpico, I. D. Mayergoyz, and G. Bertotti, *J. Appl. Phys.* **93**, 6909–6911 (2003).
- ²⁰A. V. Kimel, A. Kirilyuk, P. A. Usachev, R. V. Pisarev, A. M. Balbashov, and Th. Rasing, *Nature* **435**, 655–657 (2005).